

## Research Article

Xiaoping Wu\* and Yong Liu

# Microstructure of metatitanic acid and its transformation to rutile titanium dioxide

<https://doi.org/10.1515/htmp-2020-0097>

received January 16, 2020; accepted October 01, 2020

**Abstract:** The microstructure of metatitanic acid and its transformations to titanium dioxide during calcination have been investigated previously. However, the detailed microstructure of metatitanic acid has not been elucidated. Herein, we report the high-resolution scanning electron microscopy and X-ray powder diffraction determinations of the microstructure of metatitanic acid and its transformation to titanium dioxide during calcination. It is the first time that the detailed microstructure of metatitanic acid and its transformation to rutile titanium dioxide during calcination have been observed and elucidated. A mechanism of the transformation from metatitanic acid to crystalline titanium dioxide during calcination is described. The basic building blocks of metatitanic acid are the ultrafine crystals with an averaged diameter of a few nanometres, and these ultrafine crystals aggregate to form the porous primary particles. The primary particles further agglomerate to form the porous secondary particle. During the calcination, metatitanic acid undergoes size enlargement of ultrafine crystals, anatase–rutile transformation, merge of primary particles, and the crystal growth of titanium dioxide.

**Keywords:** microstructure, metatitanic acid, titanium dioxide

## 1 Introduction

Titanium dioxide is an important inorganic material that has a wide range of applications such as pigment and functional materials in energy and environmental areas [1–6]. One of the most common methods for the commercial production of titanium dioxide is the sulphate process [7,8]. In the sulphate process, ilmenite ( $\text{FeTiO}_3$ ) or slag reacts with the concentrated sulphuric acid in the reaction:  $\text{FeTiO}_3(\text{s}) + 2\text{H}_2\text{SO}_4(\text{aq}) = \text{TiOSO}_4(\text{aq}) + \text{FeSO}_4(\text{aq}) + 2\text{H}_2\text{O}$ . The resulting solution contains titanyl sulphate ( $\text{TiOSO}_4$ ) and ferrous sulphate ( $\text{FeSO}_4$ ). The addition of iron into the solution is necessary to reduce  $\text{Fe}^{3+}$  to  $\text{Fe}^{2+}$ , so that  $\text{Fe}^{2+}$  will remain in the solution. After a series of precipitation, removal of sulphate heptahydrate ( $\text{FeSO}_4 \cdot 7\text{H}_2\text{O}$ ), and solution concentration steps, the titanyl sulphate solution is hydrolysed by heating and diluting with water, and a hydrated titanium dioxide (general formula  $\text{TiO}_2 \cdot n\text{H}_2\text{O}$ ) precipitates. The hydrolysis is accelerated by adding the small amount of seeds to the feed solution. The most common form of hydrated titanium dioxide produced by the hydrolysis of the titanyl sulphate in the sulphate process is metatitanic acid ( $\text{TiO}_2 \cdot \text{H}_2\text{O}$  or  $\text{H}_2\text{TiO}_3$ ). Metatitanic acid is an important inorganic precursor for making a number of important materials such as titanium dioxide white pigment, titanium dioxide nanomaterials, and other functional materials [9–11]. The precipitated metatitanic acid is believed to consist of ultrafine particles with the large surface area. However, despite a large number of studies, the detailed structure of metatitanic acid has not yet been elucidated [9,12–18].

The transformation of metatitanic acid to rutile titanium dioxide is through a calcination process. The transformation usually goes through a number of stages: dehydration (100–500°C), desulfurisation (600–800°C), and the conversion of anatase phase of titanium dioxide to rutile phase (800–1,000°C) [19–21]. Rutile seeds are used to produce rutile pigment. The optimised particle size of pigmentary rutile titanium dioxide particles is

\* Corresponding author: Xiaoping Wu, Department of Titanium Chemical Engineering, Ansteel Research Institute of Vanadium & Titanium (Iron & Steele), State Key Laboratory of Vanadium and Titanium Resources Comprehensive Utilization, Sichuan, Panzhihua, 617000, China, e-mail: 13308173290@163.com

Yong Liu: Research Center for Environmental Science & Technology, Institute of Fundamental and Frontier Sciences, University of Electronic Science and Technology of China, Chengdu, 611731, China

around 250 nm or between 200 and 300 nm, as these particles have optimised light-scattering property of titanium dioxide pigments [7,8]. To a large extent, the morphology, the structure, and the particle size of metatitanic acid determine the structure and the pigmentary quality of calcined titanium dioxide.

Herein, we report a scanning electron microscopy (SEM) and X-ray powder diffraction (XRD) observation of the microstructure of metatitanic acid and its transformation to titanium dioxide during heating treatment from ambient temperature to 1,000°C. It is the first time that the detailed microstructure of metatitanic acid has been observed using a high resolution of SEM. The morphological changes, the anatase-rutile transformation, and the crystal growth of titanium dioxide during calcination have been investigated using SEM and XRD techniques.

## 2 Experimental

### 2.1 Materials

Metatitanic acid was obtained from an industrial source. The metatitanic acid generally contains about 40–60% water, a few percent of rutile seeds, and a small amount of inorganic compounds such as potassium compound ( $K_2O$  of 0.40 wt% to  $TiO_2$ ), phosphate compound ( $P_2O_5$  of 0.20 wt% to  $TiO_2$ ), and zinc compound ( $ZnO$  of 0.20 wt% to  $TiO_2$ ). Metatitanic acid was air dried at ambient temperature.

### 2.2 Methods

The dried metatitanic acid is grinded into fine powder for SEM and XRD measurement. The calcination of metatitanic acid was carried out in a furnace. After calcination of metatitanic acid at different temperatures, the samples were grinded into fine powder. The microstructure and morphologies of the metatitanic acid and its calcined samples were characterised by SEM (SEM model: ZEISS Sigma 500). The particle size of crystallites and crystal phases were determined by XRD (diffractometer model: PANalytical/EMPYREAN, The Netherlands) operating in a transmission mode with  $Cu\ K\alpha$  radiation ( $\lambda = 1.5418\text{ \AA}$ ). The quantitative analysis of anatase and rutile phases was conducted by using the method of Rietveld whole

pattern fitting [22]. The mass fractions of anatase phase ( $w_{ra}$ ) and rutile phase ( $w_{rr}$ ) were first determined using the Rietveld whole pattern fitting method, and the contents of anatase  $TiO_2$  ( $w_a$ ) and rutile  $TiO_2$  ( $w_r$ ) were then calculated by using equations

$$w_a = w_{ra}/(w_{ra} + w_{rr}) \times 100\% \text{ and } w_r = 100 - w_a$$

The average size of the ultrafine crystals was determined based on the Scherrer equation [23]:

$$D_{hkl} = 0.9\lambda/(\beta_{1/2} \cos \theta),$$

where  $D_{hkl}$  = crystallite dimension normal to the  $hkl$  reflecting planes,  $\lambda$  = X-ray wave length,  $\beta_{1/2}$  = half-maximum line breadth, and  $\theta$  = Bragg angle.

## 3 Results and discussion

### 3.1 Microstructure of metatitanic acid

Figure 1 shows a SEM image of metatitanic acid powder (30k $\times$  magnifications). The particles in the image are secondary particles of metatitanic acid with the particle size of a few hundreds of nanometres. This type of images of metatitanic acid has been observed in a number of previous studies [24–26]. However, when the metatitanic acid was observed under exceptional magnifications (over 400k $\times$  magnifications), the fine microstructure of metatitanic acid is revealed, as shown in Figure 2.

It is shown in Figure 2 that metatitanic acid consists of secondary particles with a particle diameter of a few hundred nanometres (red cycle in Figure 2). A secondary

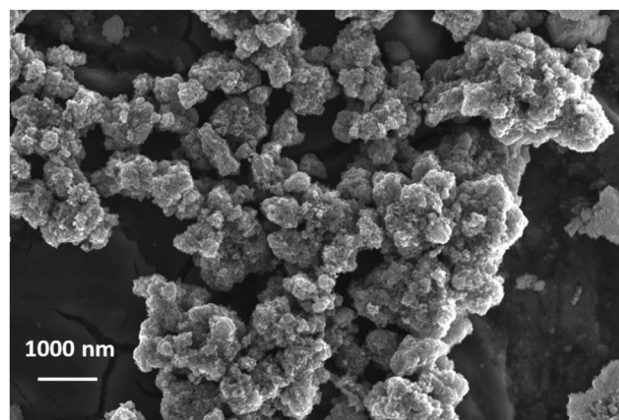


Figure 1: SEM image of metatitanic acid (30k $\times$  magnifications).

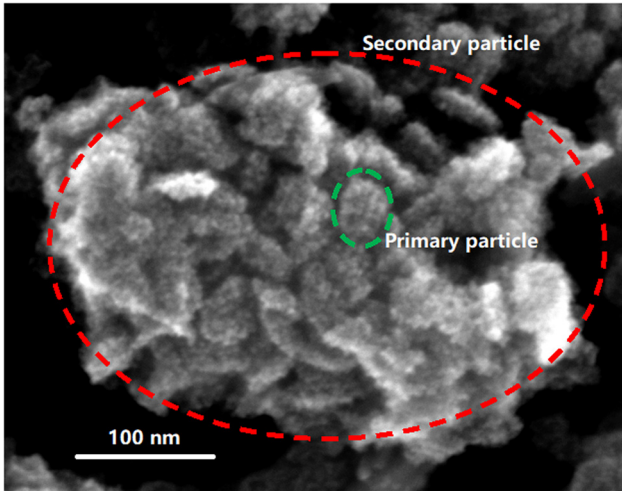


Figure 2: SEM image of metatitanic acid (419.78k× magnifications).

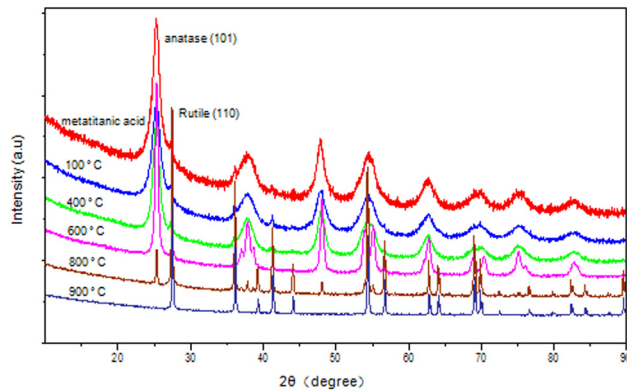


Figure 3: XRD patterns of metatitanic acid and its calcined samples at different temperatures.

particle is the agglomeration of the primary particles that have the averaged diameters of tens of nanometres (green cycle in Figure 2). The internal structure of a primary particle under the high resolution of SEM can be further observed to consist of ultrafine particles with a diameter less than 10 nm. A XRD determination shows that ultrafine particles inside primary particles are anatase crystals with a size of around 5 nm.

### 3.2 Transformation of metatitanic acid to TiO<sub>2</sub>

Figure 3 shows the XRD pattern of metatitanic acid after heating treatment at different temperatures. At 100°C, the XRD pattern is the same as metatitanic acid at ambient temperature. The small peak of the rutile phase (in

Table 1: Size changes of particles inside metatitanic acid

	100°C	400°C	600°C	800°C	900°C
$D_u$ (nm)	6.0	9.0	23.0	62.0	—
$D_p$ (nm)	72.0	75.0	56.0	—	—
$D_s$ (μm)	1.0	1.0	0.9	—	—

$D_u$ : particle size of ultrafine crystals in metatitanic acid (by XRD);  $D_p$ : particle size of primary particles (by SEM);  $D_s$ : particle size of secondary particles (by SEM).

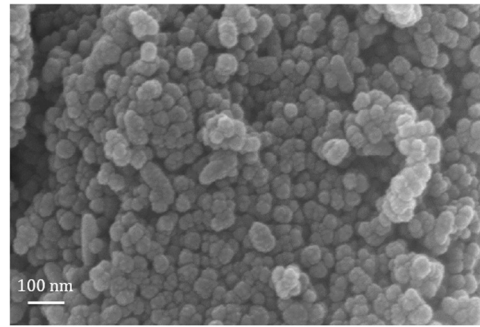
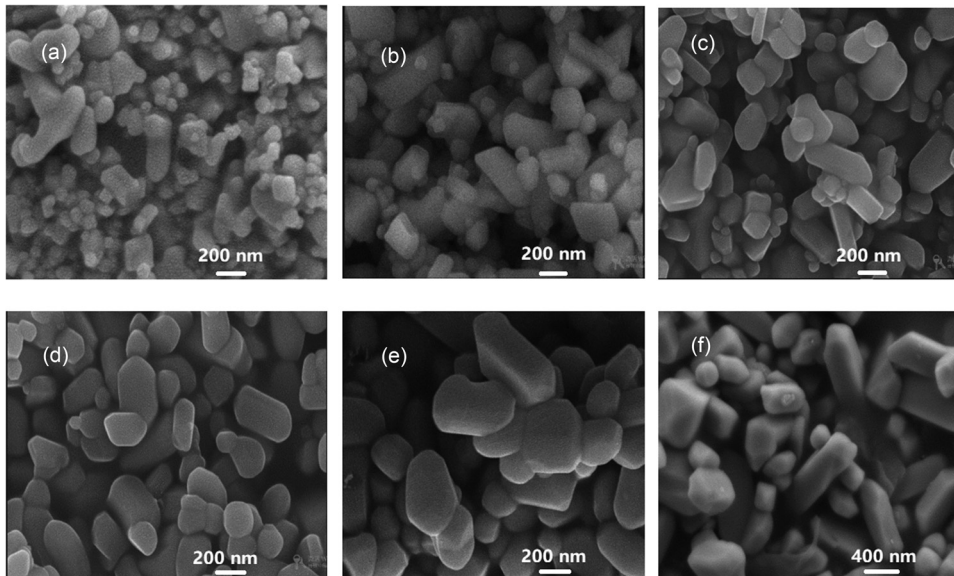


Figure 4: Primary particles of metatitanic acid after heating treatment at 750°C.

metatitanic acid) is due to the addition of rutile seeds for producing rutile titanium dioxide. The particle size of anatase ultrafine crystals is determined to be 6 nm. As the calcination temperature increases, the particle size of anatase ultrafine crystals increases (Table 1), and the anatase–rutile transformation become significant at 800°C.

The interactions between particles that constitute the secondary and primary particle are also observed to be different. As shown in Figure 4, after heating at 750°C for an hour, the secondary particles largely disintegrated into primary particles, but the integrity of primary particles remains. This confirms that the secondary particles are the agglomeration of the primary particles, and the interactions between primary particles in a secondary particle are physical and relatively weak. The interactions between microcrystals inside a primary particle are of a degree of chemical interaction and relatively strong.

Table 1 summaries the size changes of particles, which constitute metatitanic acid in the heating treatment at different temperatures. As the temperature increases over 400°C, the particle size of ultrafine crystals increases rapidly. At 800°C, the particle size increases to 62 nm. The sizes of the primary and secondary particles remain fairly constant up to 400°C. After 600°C, these sizes become smaller.



**Figure 5:** Morphology changes and crystal growth of metatitanic acid during calcination. (a) 800°C, (b) 830°C, (c) 845°C, (d) 850°C, (e) 900°C, (f) 1000°C.

**Table 2:** Averaged particle size and anatase–rutile transformation rate of metatitanic acid during calcinations

SEM image	Temperature (°C)	Averaged particle size (nm)	A–R transformation rate (%)
(a)	800	146	51.7
(b)	830	224	90.7
(c)	845	231	95.7
(d)	850	252	99.1
(e)	900	382	100.0
(f)	1,000	772	100.0

Park and Shin studied the specific surface areas and pore volumes of metatitanic acid after heating treatment at different temperatures [27]. The BET-specific surface areas ( $A_{\text{BET}}$ ,  $\text{m}^2/\text{g}$ ) and pore volumes ( $V$ ,  $\text{cm}^3/\text{g}$ ) of heat-treated metatitanic acid at 100°C are around 377 and 0.297, respectively. This is consistent with our observation that a primary particle of metatitanic acid consist of ultrafine crystals and is porous. The previous thermal analysis and XRD studies [24–26] have demonstrated that after heating over 100°C, metatitanic acid begin to loss water: initially, free water,  $\text{H}_2\text{O}(\text{l}) \rightarrow \text{H}_2\text{O}(\text{g})$ , and

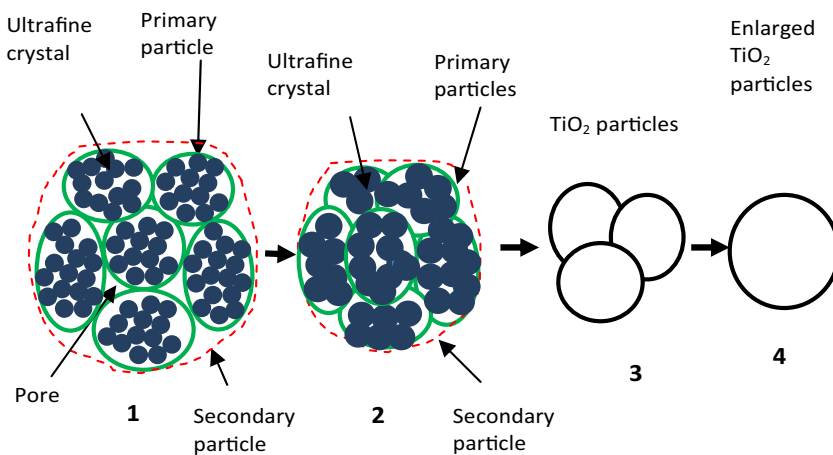


**Figure 6:** The mechanism of the transformation from metatitanic acid to crystalline titanium dioxide during calcination.

then hydrated water at higher temperature up to 500°C:  $\text{TiO}(\text{OH})_2(\text{s}) \rightarrow \text{TiO}_2(\text{s}) + \text{H}_2\text{O}(\text{g})$ . In this study, the combined SEM and XRD investigation show that at 800°C, metatitanic acid has already transformed into a mixture of anatase and rutile titanium dioxide particles (see Figure 5(a) and Table 2). At the temperature over 800°C, smaller particles coalesce further to form larger particles, and at the same time, anatase continues to transform into the rutile phase (Figure 5(b, c) and Table 2). The agglomerated secondary particles of metatitanic acid have disintegrated, and the size of primary particles of metatitanic acid increase rapidly. At the same time, rutile content of titanium dioxide increase. At 850°C, the anatase–rutile transformation is almost complete, and the particles of rutile titanium dioxide reach an optimum averaged size of around 250 nm (Figure 5(d) and Table 2). At the higher temperatures, rutile titanium dioxide particles coalesce into even larger particles (Figure 5(e, f) and Table 2).

From the aforementioned studies and analysis, the mechanism of the transformation from metatitanic acid to crystalline titanium dioxide during calcination is shown as in Figure 6: **1**, the original microstructure of metatitanic acid; **2**, dehydrated intermediate, with the increased size of ultrafine crystals; **3**,  $\text{TiO}_2$  pigment particles after anatase–rutile transformation and crystal growth; **4**, further merged and grew  $\text{TiO}_2$  particles after prolonged heating at high temperature.

## 4 Conclusion

We have observed and determined the detailed microstructure of metatitanic acid using the high-resolution SEM and XRD. The basic building blocks of the metatitanic acid are the anatase ultrafine crystals with an average size of around 5 nm. These ultrafine crystals aggregate to form the porous primary particles with an average diameter of a few tens of nanometres. The primary particles further agglomerate to form the secondary porous particles with an average diameter of a few hundreds of nanometres. During calcination, the particle size of anatase ultrafine crystals increases continuously. After reaching 800°C, the primary particles begin to merge together, and at the same time, the anatase–rutile transformation become significant. At 850°C, the merge of primary particles complete, and anatase–rutile transformation reach about 100%. This point represents an optimised particle size of pigmentary titanium dioxide. Furthermore, prolonged calcination at high temperature leads to coalesce and increases the chances of rutile

titanium dioxide particles to form larger particles. A mechanism of the transformation from metatitanic acid to crystalline titanium dioxide during calcination is described.

**Acknowledgments:** This work was financially supported by the Pangang Group under a Basic Research Grant. We thank Dr Zhaohua Liu, Mr Zhixin Shi, and Mr Xibin Liu for SEM and X-ray diffraction analyses, experimental help, and discussion.

**Conflict of interest:** There are no conflicts to declare.

## References

- [1] O'Regan, B., and M. Gratzel. A low-cost, high-efficiency solar cell based on dye-sensitized colloidal  $\text{TiO}_2$  films. *Nature*, Vol. 353, 1991, pp. 737–740.
- [2] Kay, A., and M. Gratzel. Artificial photosynthesis. 1. Photosensitization of titania solar cells with chlorophyll derivatives and related natural porphyrins. *The Journal of Physical Chemistry*, Vol. 97, 1993, pp. 6272–6277.
- [3] Fujishima, A., and K. Honda. Electrochemical photolysis of water at a semiconductor electrode. *Nature*, Vol. 238, 1972, pp. 37–38.
- [4] Fujishima, A., T. N. Rao, and D. A. Tryk. Titanium dioxide photocatalysis. *Journal of Photochemistry and Photobiology C*, Vol. 1, 2000, pp. 1–21.
- [5] Tryk, D. A., A. Fujishima, and K. Honda. Recent topics in photoelectrochemistry: achievements and future prospects. *Electrochimica Acta*, Vol. 45, 2000, pp. 2363–2367.
- [6] Chen, X., and S. S. Mao. Titanium dioxide nanomaterials: synthesis, properties, modifications, and applications. *Chemical Reviews*, Vol. 107, 2007, pp. 2891–2959.
- [7] Winkler, J. *Titanium dioxide, production, properties and effective usage*, 2nd edn. Vincentz Network, Hanover, 2013.
- [8] Lakshmanan, V. I., A. Bhowmick, and M. A. Halim. In *Titanium dioxide, chemical properties, applications and environmental effects*, J. Brown, Eds, Nova Science Publishers, New York, 2014, pp. 75–130.
- [9] Gesenhues, U. Calcination of metatitanic acid to titanium dioxide white pigments. *Chemical Engineering & Technology*, Vol. 24, 2001, pp. 685–694.
- [10] Song, H., H. B. Liang, L. Lu, P. Wu, and C. Li. Effect of hydrolysis conditions on hydrous  $\text{TiO}_2$  polymorphs precipitated from a titanyl sulfate and sulfuric acid solution. *International Journal of Minerals, Metallurgy and Materials*, Vol. 19, 2002, pp. 642–650.
- [11] Xu, R., J. Li, Z. Tang, and Z. Zhang. Ultrafine metatitanic acid electrode for ultrafast lithium ion batteries. *Electrochimica Acta*, Vol. 56, 2011, pp. 6330–6335.
- [12] Li, Z., Z. Wang, and G. Li. Preparation of nano-titanium dioxide from ilmenite using sulfuric acid-decomposition by liquid

- phase method. *Powder Technology*, Vol. 287, 2016, pp. 256–263.
- [13] Jalava, J., L. Heikkilä, O. Hovi, R. Laiho, E. Hiltunen, A. Hakanen, et al. Structural investigation of hydrous TiO<sub>2</sub> precipitates and their aging products by X-ray diffraction, atomic force microscopy, and transmission electron microscopy. *Industrial & Engineering Chemistry Research*, Vol. 37, 1998, pp. 1317–1323.
- [14] Jalava, J., E. Hiltunen, H. Kähkönen, H. Erkkilä, H. Härmä, and V. Taavitsainen. Structural investigation of hydrous titanium dioxide precipitates and their formation by small-angle X-ray scattering. *Industrial & Engineering Chemistry Research*, Vol. 39, 2000, pp. 349–361.
- [15] Bavykin, D. V., V. P. Dubovitskaya, A. V. Vorontsov, and V. N. Parmon. Effect of TiOSO<sub>4</sub> hydrothermal hydrolysis conditions on TiO<sub>2</sub> morphology and gas-phase oxidative activity. *Research on Chemical Intermediates*, Vol. 33, 2007, pp. 449–464.
- [16] Denisova, T. D., G. Maksimova, E. V. Polyakov, N. A. Zhuravlev, S. A. Kovyazina, O. N. Leonidova, et al. Metatitanic acid: synthesis and properties, *Russian Journal of Inorganic Chemistry*, Vol. 51, 2006, pp. 691–699.
- [17] Grzmil, B. U., D. Grela, and B. Kic. Hydrolysis of titanium sulphate compounds. *Chemical Papers*, Vol. 62, 2008, pp. 18–25.
- [18] Nosaka, Y., and A. Nosaka. *Introduction to photocatalysis, from basic science to application*. Royal Society of Chemistry, Cambridge, 2016.
- [19] Sullivan, W. F., and S. S. Cole. Thermal chemistry of colloidal titanium dioxide. *Journal of the American Ceramic Society*, Vol. 42, 1959, pp. 127–133.
- [20] Ginsberg, T., M. Modigell, and W. Wilsmann. Thermochemical characterisation of the calcination process step in the sulphate method for production of titanium dioxide. *Chemical Engineering Research and Design*, Vol. 89, 2011, pp. 990–994.
- [21] Tian, C., Y. Yang, and H. Pu. Effect of calcination temperature on porous titania prepared from industrial titanyl sulfate solution. *Applied Surface Science*, Vol. 257, 2011, pp. 8391–8395.
- [22] Dong, W., C. Gilmore, G. Barr, C. Dallman, N. Feeder, and S. Terry. A Quick method for the quantitative analysis of mixtures. 1. Powder X-ray diffraction. *Journal of Pharmaceutical Technology*, Vol. 97, 2008, pp. 2260–2276.
- [23] Chung, F. H., and D. K. Smith. *Industrial Application of X-Ray Diffraction*. Marcel Dekker, New York, 2000.
- [24] Sathyamoorthy, S., G. D. Moggridge, and M. J. Hounslow. Particle formation during anatase precipitation of seeded titanyl sulfate solution. *Crystal Growth & Design*, Vol. 1, 2001, pp. 123–129.
- [25] Santacesaria, E., M. Tonello, G. Storti, R. C. Pace, and S. Carra. Kinetics of titanium dioxide precipitation by thermal hydrolysis. *Journal of Colloid and Interface Science*, Vol. 111, 1986, pp. 44–53.
- [26] Zhang, W., C. Ou, and Z. Yuan. Precipitation and growth behaviour of metatitanic acid particles from titanium sulfate solution. *Powder Technology*, Vol. 315, 2017, pp. 31–36.
- [27] Park, S., and H. Shin. Microstructural evolution of metatitanic acid with temperature and its photosensitization property. *Reaction Kinetics, Mechanisms and Catalysis*, Vol. 101, 2013, pp. 237–249.